

Current Biology

An Amphibious Whale from the Middle Eocene of Peru Reveals Early South Pacific Dispersal of Quadrupedal Cetaceans

Highlights

- A quadrupedal whale is described based on a skeleton from the middle Eocene of Peru
- It combines terrestrial locomotion abilities and use of the tail for swimming
- This is the first record of an amphibious whale for the whole Pacific Ocean
- It supports early dispersal of cetaceans to the New World across the South Atlantic

Authors

Olivier Lambert, Giovanni Bianucci, Rodolfo Salas-Gismondi, Claudio Di Celma, Etienne Steurbaut, Mario Urbina, Christian de Muizon

Correspondence

olivier.lambert@naturalsciences.be

In Brief

Lambert et al. describe a new cetacean from the middle Eocene of Peru, characterized by retention of terrestrial locomotion abilities and a significant contribution of the tail for swimming. This first indisputable quadrupedal whale from the Pacific Ocean supports early dispersal of amphibious cetaceans to the New World across the South Atlantic.

An Amphibious Whale from the Middle Eocene of Peru Reveals Early South Pacific Dispersal of Quadrupedal Cetaceans

Olivier Lambert,^{1,8,*} Giovanni Bianucci,² Rodolfo Salas-Gismondi,^{3,4} Claudio Di Celma,⁵ Etienne Steurbaut,^{1,6} Mario Urbina,⁴ and Christian de Muizon⁷

¹D.O. Terre et Histoire de la Vie, Institut royal des Sciences naturelles de Belgique, Rue Vautier 29, 1000 Brussels, Belgium

²Dipartimento di Scienze della Terra, Università di Pisa, Via S. Maria 53, 56126 Pisa, Italy

³BioGeoCiencias Lab, Facultad de Ciencias y Filosofía/CIDIS, Universidad Peruana Cayetano Heredia, Lima, Peru

⁴Departamento de Paleontología de Vertebrados, Museo de Historia Natural-UNMSM, Avenida Arenales 1256, 14 Lima, Peru

⁵Scuola di Scienze e Technologie, Università di Camerino, Via Gentile III da Varano 1, 62032 Camerino, Italy

⁶Department of Earth and Environmental Sciences, KU Leuven, Celestijnenlaan 200E, 3001 Leuven, Belgium

⁷Centre de Recherche en Paléontologie-Paris, CR2P (CNRS, MNHN, Sorbonne-Université), Département Origines et Évolution, Muséum national d'Histoire naturelle, 8, Rue Buffon 75005 Paris, France

⁸Lead Contact

*Correspondence: olivier.lambert@naturalsciences.be

<https://doi.org/10.1016/j.cub.2019.02.050>

SUMMARY

Cetaceans originated in south Asia more than 50 million years ago (mya), from a small quadrupedal artiodactyl ancestor [1–3]. Amphibious whales gradually dispersed westward along North Africa and arrived in North America before 41.2 mya [4]. However, fossil evidence on when, through which pathway, and under which locomotion abilities these early whales reached the New World is fragmentary and contentious [5–7]. *Peregocetus pacificus* gen. et sp. nov. is a new protocetid cetacean discovered in middle Eocene (42.6 mya) marine deposits of coastal Peru, which constitutes the first indisputable quadrupedal whale record from the Pacific Ocean and the Southern Hemisphere. Preserving the mandibles and most of the postcranial skeleton, this unique four-limbed whale bore caudal vertebrae with bifurcated and anteroposteriorly expanded transverse processes, like those of beavers and otters, suggesting a significant contribution of the tail during swimming. The fore- and hind-limb proportions roughly similar to geologically older quadrupedal whales from India and Pakistan, the pelvis being firmly attached to the sacrum, an insertion fossa for the round ligament on the femur, and the retention of small hooves with a flat anteroventral tip at fingers and toes indicate that *Peregocetus* was still capable of standing and even walking on land. This new record from the southeastern Pacific demonstrates that early quadrupedal whales crossed the South Atlantic and nearly attained a circum-equatorial distribution with a combination of terrestrial and aquatic locomotion abilities less than 10 million years after

their origin and probably before a northward dispersal toward higher North American latitudes.

RESULTS

Systematics

Cetacea

Protocetidae

Peregocetus pacificus gen. et sp. nov.

Etymology

Peregocetus from Latin *pereger* (travel abroad) and *cetus* (whale); *pacificus* for the Pacific Ocean; the traveling whale that reached the Pacific Ocean.

Holotype

Museo de Historia Natural, Universidad Nacional Mayor de San Marcos (MUSM, Lima, Peru) 3580, a partial skeleton including the mandibles and teeth; thoracic, lumbar (at least 5), sacral, and caudal (at least 12) vertebrae; ribs, sternal elements (including manubrium and xiphisternum), scapulae, humeri, radii, ulnae, carpals, metacarpals, and manus phalanges; innominate, femora, tibia, fibula, tarsals (including astragali and calcanei), metatarsals, and pes phalanges (Figures 1, 2, and S2).

Locality

Playa Media Luna, southern part of Pisco Basin, southern coast of Peru, 14° 36' 14.7" S, 75° 54' 48.5" W (Figure S1), 220 m south to the locality of the holotype of *Mystacodon selenensis* [9].

Horizon

Lowest part of the Yumaque Member, 1.95 m above the base; upper part of calcareous nannofossil Zone CNE13 of Agnini et al. [10], approximately 42.6 mya, middle Eocene (early late Lutetian; see Figure S1, Table S1, and STAR Methods for the biostratigraphic and biochronological interpretations).

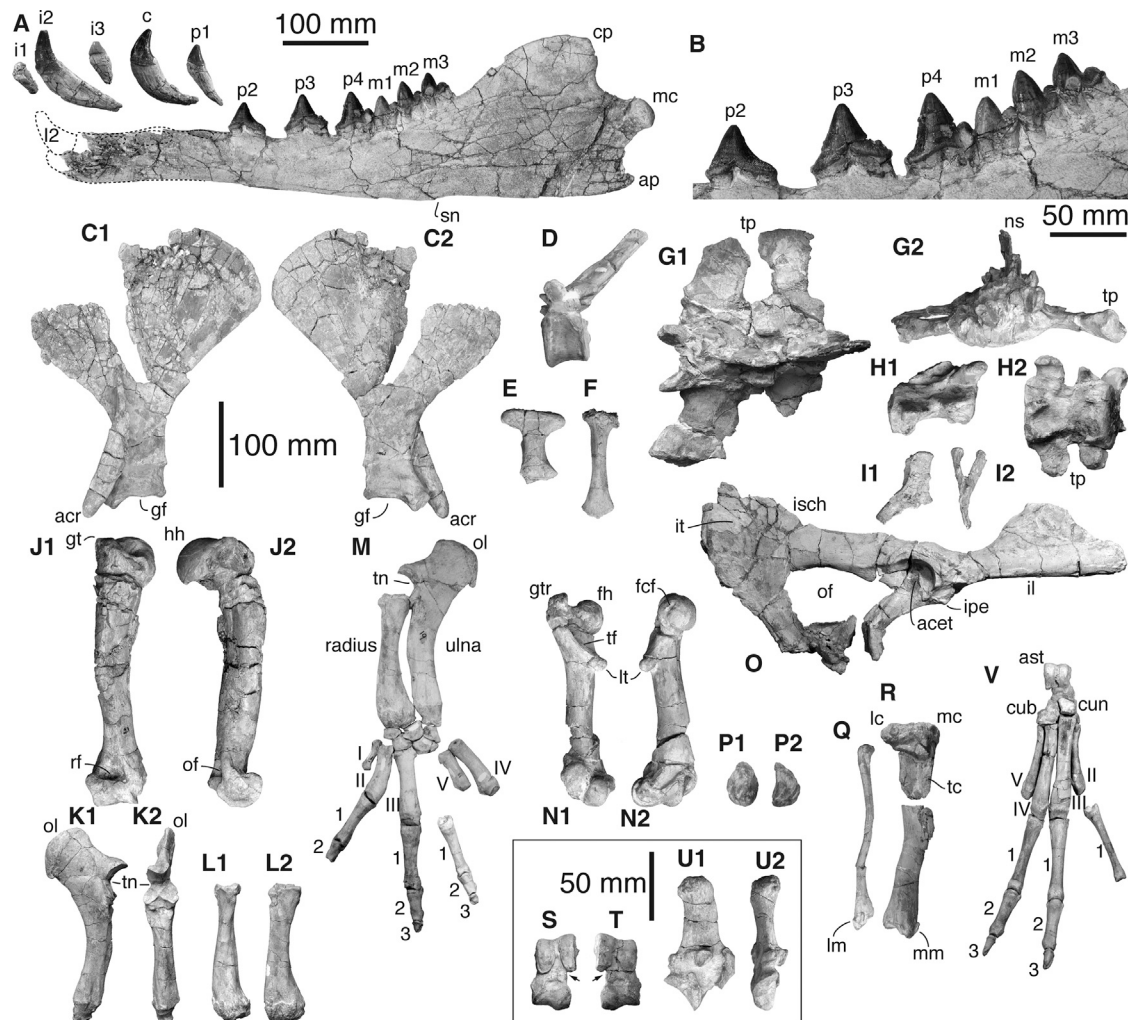


Figure 1. Mandible and Postcranial Bones of *Peregocetus pacificus* gen. et sp. nov. MUSM 3580 (Holotype)

(A) Left mandible in lateral view, together with corresponding detached anterior teeth. Stippled anterior part based on right mandible.

(B) Detail of the posterior lower cheek in lateral view.

(C1 and C2) Left scapula in lateral (C1) and medial (C2) view.

(D) Thoracic vertebra in left lateral view.

(E and F) Sternal elements: manubrium (E) and xiphisternum (F) in ventral view.

(G1 and G2) Sacral vertebrae S1–S2 in dorsal (G1) and anterior (G2) view.

(H1 and H2) Anterior caudal vertebra in right lateral (H1) and ventral (H2) view.

(I1 and I2) Chevron in right lateral (I1) and anterior view (I2).

(J1 and J2) Right humerus in anterior (J1) and lateral (J2) view.

(K1 and K2) Left ulna in medial (K1) and anterior (K2) view.

(L1 and L2) Left radius in posterior (L1) and lateral (L2) view.

(M) Left radius, ulna, and manus in lateral view. Metatarsals IV and V are from right manus.

(N1 and N2) Left femur in posterior (N1) and medial (N2) view.

(O) Right innominate in lateral view.

(P1 and P2) Patella in anterior (P1) and medial/lateral (P2) view.

(Q) Right fibula in anterior view.

(R) Right tibia in anterior view.

(S and T) Left (S) and right (T) astragali in anterior view. Arrows point to a distinct notch on lateral margin.

(U1 and U2) Right calcaneum in medial (U1) and anterior (U2) view.

(V) Right pes in anterior view.

1–5, manus and pes phalanges; acet, acetabulum; acr, acromion; ap, angular process; ast, astragalus; cp, coronoid process; cub, cuboid; cun, cuneiform; fcf, fovea capitis femoris; gf, glenoid fossa; gt, greater tuberosity; gtr, greater trochanter; hh, humeral head; I–V, metacarpals and metatarsals; il, ilium; ipe, iliopectinal eminence; isch, ischium; it, ischiatic table; lc, lateral condyle; lm, lateral malleolus; lt, lesser trochanter; mc, medial condyle; mm, medial alveolus; of, obturator foramen; ol, olecranon; mc, mandibular condyle; sn, step-like notch; tc, tibial crest; tf, trochanteric fossa; tp, transverse process; ns, neural spine.

See also [Figure S2](#) and [Data S2](#).

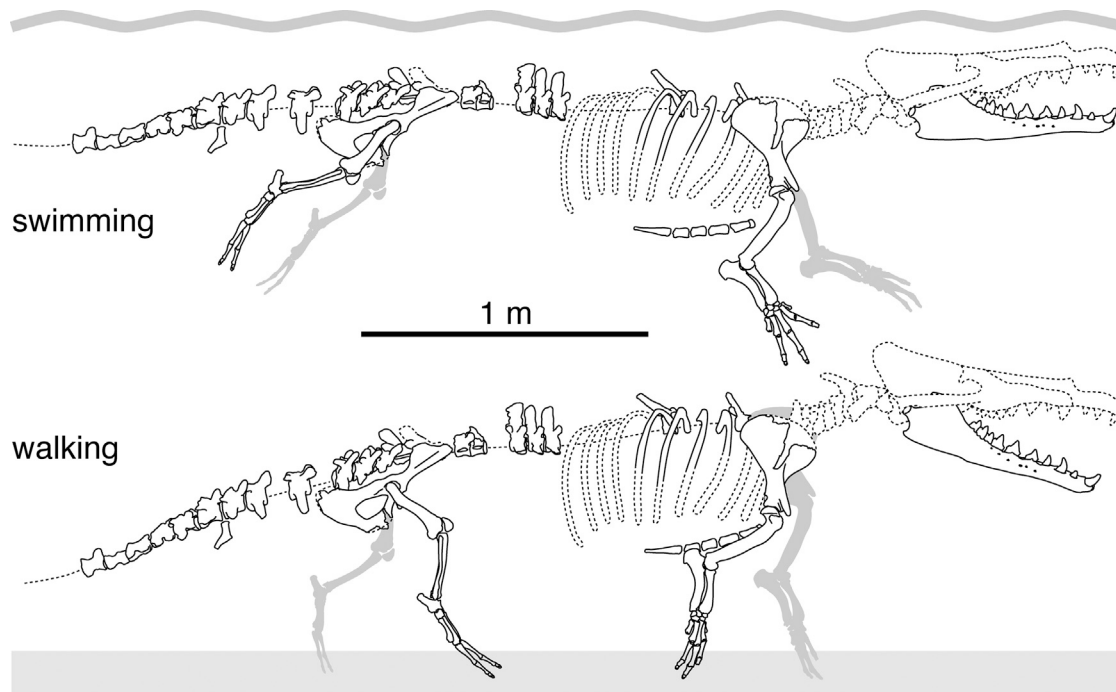


Figure 2. Preserved Parts of the Skeleton of *Peregocetus pacificus* gen. et sp. nov. MUSM 3580 (Holotype).

Schematic drawings of the articulated skeleton of MUSM 3580 showing the main preserved bones, in a hypothetical swimming and terrestrial posture. For paired bones, the best-preserved side was illustrated (sometimes reversed), or both sides were combined (e.g., mandible). Stippled lines indicate reconstructed parts and missing sections of the vertebral column; cranium, cervical vertebrae, and ribs based on *Maiacetus inuus* [8]. See also [Figures S2](#) and [S4](#) and [Data S2](#).

Diagnosis

MUSM 3580 is a member of the paraphyletic group Protocetidae due to molars with identifiable trigonid (formed by protoconid) and talonid (formed by hypoconid), accessory denticles absent on cheek teeth; fewer than four fused sacral vertebrae; radius not transversely flattened; articulation of innominate with sacrum present; functional hind limbs, with femur only 18% shorter than humerus; and trapezoid and magnum unfused [6, 11–13]. It differs from all other protocetids in the following unique combination of characters: unfused mandibular symphysis, ending just anterior to p3; ratio between height of mandible at coronoid process and height at anterior margin of p4 nearly equals 2.7; dorsal margin of mandibular condyle at vertical level of posterior margin of alveolus for m3; angular process of the mandible distinctly pointed; only slightly convex ventral margin of the angular process, preceded anteriorly by step-like notch, at level of m3; markedly ornamented enamel on all teeth; small single-rooted p1; short diastema between p3 and p4 and no diastema between p4 and m1; p4 bearing a large distal cusp; absence of metaconid on lower molars; two fused sacral vertebrae; ilium triangular in lateral view, with an anteriorly projected anteroventral spine; ventromedial expansion of pubis ventral to obturator foramen moderate; and well-defined fovea capitis femoris.

Additional Descriptive Elements

Dimensions of the mandible, cheek teeth, and postcranial elements of MUSM 3580 (see [Data S2](#)) indicate a large protocetid, approximately 4 m long, close in size to *Georgiacetus*, larger than *Maiacetus* and *Rodhocetus* but smaller than *Pappocetus*

[1, 8, 11, 14]. Considering that all vertebral and limb bone epiphyses are firmly attached to centra and diaphyses, respectively, this specimen is interpreted as fully adult.

On the mandible, the high coronoid process ends posteriorly before the condyloid neck ([Figures 1](#) and [S2](#)). The latter is shorter than in *Carolinacetus* [6]. The pointed tip of the angular process nearly reaches the anterior level of the condyle. A step-like notch on the ventral margin is also observed in *Pappocetus* and, to a lesser extent, *Crenatocetus* [12]. The anterior margin of the large mandibular foramen is sub-rectilinear, directed anteroventrally, and reaching a level intermediate between the top of the coronoid process and m3. The outline of the anterior part of the mandible in lateral view indicates the absence of clinorhynch (*sensu* [15]).

The i1 is considerably reduced, with i2 being the largest incisor and i3 being close in size to the small single-rooted p1. The distal carina of p2 is distinctly concave in lateral view. The p3 is the longest lower tooth, and it bears a distal cusp much smaller than on p4, where the cusp approximates the size of the large hypoconid on m1–m3. The mesial carina of p4 draws an angle <20° with the vertical, being more erected than in *Aegyptocetus*, *Kharodacetus*, and *Crenatocetus*. Each lower molar displays a vertical notch in the mesial edge. The m3 is the longest molar. Enamel is markedly ornamented on the crown of each preserved tooth, as in *Crenatocetus*, *Georgiacetus*, and *Pappocetus* [12]. Apical wear is incipient in all the preserved teeth.

The manubrium (first sternal element) is T shaped, as in several other protocetids and in the basilosaurid *Supayacetus* [16]. The acromion of the scapula is slender and directed distally. The

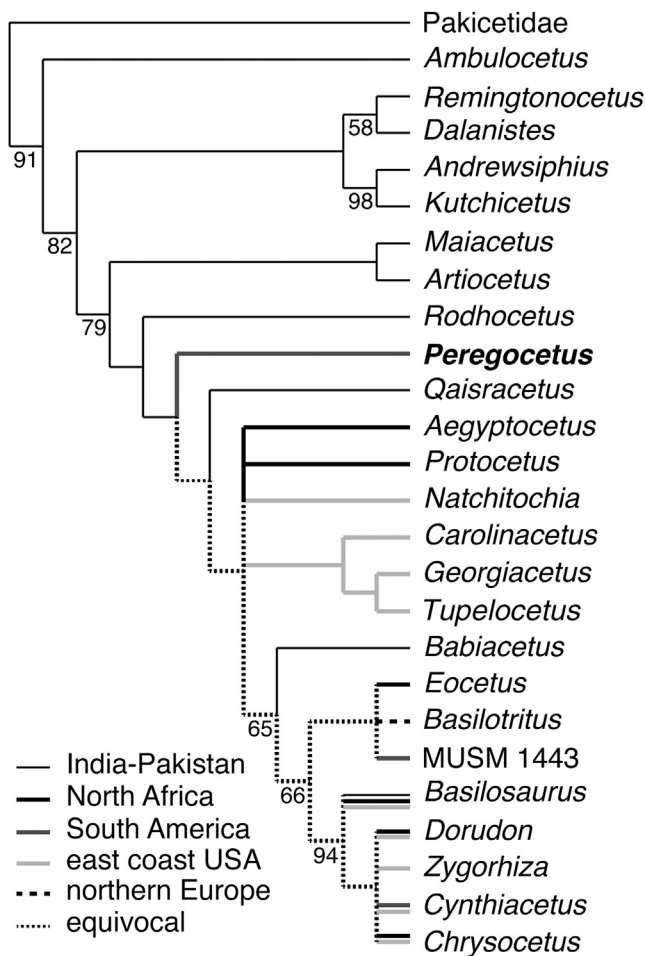


Figure 3. Phylogenetic Relationships of *Peregocetus pacificus* gen. et sp. nov.

Consensus tree of the heuristic search with homoplastic characters down-weighted, showing the relationships of *P. pacificus* with other archaeocetes. Numbers correspond to bootstrap values >50. Different line styles indicate the main geographic areas from where the taxa originate and the main dispersal events, as obtained from a simple optimization of the main localities on the consensus tree. See also [Figure S3](#) and [Data S1](#).

humerus is long, with proportions close to *Maiacetus* [8]. The head is large and hemispherical, extending barely farther proximally than the small greater tuberosity. The deltopectoral crest is poorly developed. Both the olecranon and radial fossae are deep, indicating a high range of flexion and extension for the elbow. The ulna is shorter than the humerus. The robust olecranon process displays a thickened distal surface for the insertion of triceps brachii. Distal to the trochlear notch, a rough surface on the medial surface of each ulna corresponds to an attachment area for biceps brachii and/or brachialis. The distal epiphysis of the ulna is truncated and bears a flat articulation with the cuneiform. The transverse articulation of the proximal epiphysis of the radius with the humerus and its flat and circular facets with the ulna indicate that pronation-supination movements were unlikely. Ulna and radius are less curved in lateral view than in *Maiacetus*. The manus includes five fingers. The ratio of midshaft width to length for metacarpal III is 0.20, corre-

sponding to a manus more robust than in *Ambulocetus*, *Maiacetus*, and *Pakicetus* and closer to *Rodhocetus* [1, 2]. The third digit is as long as the forearm, being shorter than in *Ambulocetus* and similar to *Maiacetus*. Preserved last phalanges indicate the presence of small hooves.

Sacral vertebrae S1 and S2 are completely fused at the level of the centrum, as in *Qaisracetus*. An additional sacral centrum is preserved, probably representing the third unfused sacral vertebra (i.e., first sacral caudal vertebra Sca1). Incomplete transverse processes of S1 project anterolaterally and slightly ventrally, displaying a marked dorsoventral thickening. On the triangular ilium, the greater ischiatic notch is deeply concave, as in *Maiacetus*. The medial surface of each ilium is marked by a large and deep auricular surface, for the articulation with sacral S1 ([Figures 1 and S2](#)). The iliopectinal eminence is well developed, as in *Natchitochia* [13]. The large obturator foramen is anteriorly pointed, more than in *Georgiacetus* and *Natchitochia* [11, 13]. As in *Maiacetus*, the ischium extends posterodorsally and forms a larger ischiatic table than in *Natchitochia*, *Georgiacetus*, and *Qaisracetus*, a feature tentatively related to more efficient pelvic paddling [17]. On the well-defined acetabulum, the acetabular notch is wide between both ends of the lunate surface, as in other protocetids, and it extends as a broad groove toward the ischium side of the obturator foramen, in a way more similar to *Georgiacetus*.

Twelve proximal caudal vertebrae are preserved, with the fourth and sixth probably lacking. As in some terrestrial and semi-aquatic mammals with a long tail [18, 19] and the first caudal of *Georgiacetus* [20], Ca1–3 show unlevelled anterior and posterior epiphyses, indicating that the tail was ventrally bent just behind the sacrum, leading to a tail not as horizontal as in fully aquatic cetaceans (i.e., basilosaurids and neocetes [21]). Transverse processes are relatively flat in all preserved caudals and become distinctly wider at Ca7–8, where they are perforated by vascular foramina, as in *Natchitochia* [13]. From Ca9 and backward, preserved vertebrae display bifurcated and anteroposteriorly expanded transverse processes. Bifurcated transverse processes are similarly observed in *Castorocauda* (an early semi-aquatic mammaliaform), the marine sloth *Thalassocnus*, otters, and beavers [22, 23]; in the beaver and *Castorocauda*, this feature is associated with the expansion of a paddle-shaped tail [18, 23]. In *Maiacetus*, the anterior branch of the bifurcated transverse process is conspicuously more slender than in MUSM 3580 [8].

The spherical femoral head is lower proximally than the robust greater trochanter. The head is marked by a well-defined fovea capitis femoris for the insertion of the round ligament, as in *Maiacetus* and possibly *Pappocetus* [8, 24] but differing from *Natchitochia* and *Togocetus* [13, 25]. The trochanteric fossa is deep, and the lesser trochanter is prominent and proximomedially directed. The tibia is longer than the femur. A cross section at about one-third of its length, proximally, reveals a large medullary cavity. As in other early cetaceans, the astragalus displays the typical artiodactyl double pulley. The astragalus is proportionally shorter than in *Artiocetus*, *Maiacetus*, and *Rodhocetus*, but it bears an indentation in the lateral margin similar to the condition in *Maiacetus* [8]. The paraxonic foot bears four elongated toes. The ratio of midshaft width to length for metatarsal III is 0.14, indicating feet more robust than in *Rodhocetus*. In lateral view, each metatarsal is distinctly curved, as in *Maiacetus*. Phalanges III-2 and IV-2 display flanges along the lateral and medial sides of their

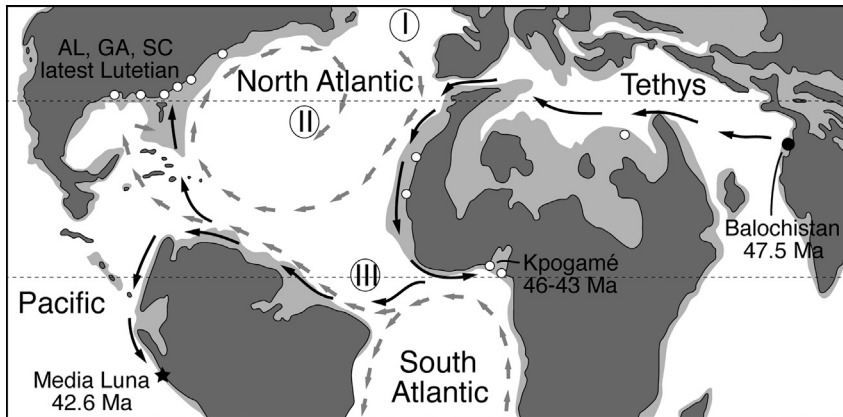


Figure 4. Distribution of Protocetid Whales during the Middle Eocene

Middle Eocene map (about 40 mya) showing land masses (dark gray), epicontinental seas (light gray), and localities for Lutetian and Bartonian protocetids (open circles). Black circle for the presumed area of origin of the group; black star for the locality of *Peregocetus pacificus* gen. et sp. nov. MUSM 3580 (holotype). I–III refer to different dispersal routes to the New World by protocetids, via northern Europe and Greenland (I), across North Atlantic (II), and across South Atlantic (III, see [7]). Black arrows illustrate our favored hypothesis, via the South Atlantic. Gray arrows indicate main Atlantic surface paleocurrents (taken from [30]). Palaeogeographic map modified from an original map by R. C. Blakey (available at deeptimemaps.com). Locality and age data from [4, 7, 8].

proximal plantar aspect, as described in *Rodhocetus* [1]. The preserved distal phalanges, presumably for toes III and IV, indicate the presence of narrow hooves. In lateral view, the apex of each distal phalanx bears a small flat surface, which makes an angle of about 45° with the long axis of the bone.

Phylogenetic Analysis and Paleobiogeography

Both heuristic searches, with and without downweighting of homoplastic characters (DHC), found *Peregocetus* as an early branch among protocetids, diverging after *Artiocetus* + *Maiacetus* and *Rodhocetus* but before *Qaisracetus* and all protocetids from outside Indo-Pakistan coded in the analyses. Among more derived protocetids, the analysis with DHC resulted in a somewhat better-resolved consensus tree, with three taxa from the East Coast United States (*Carolinacetus*, *Georgiacetus*, and *Tupelocetus*) forming a clade (Figure 3), whereas in the analysis without DHC, *Georgiacetus* appears as a separate, more crownward branch (Figure S3).

Optimization of archaeocete localities on the consensus tree of the analysis with DHC leads to the identification of at least two dispersal events within protocetids from and/or to Indo-Pakistan (Figure 3): an early westward event accounting for the presence of *Peregocetus* in South America, followed either by at least one (and possibly two) westward dispersal(s) for protocetids of North Africa and East Coast United States or, less likely, eastward dispersals, back to Indo-Pakistan, for *Qaisracetus* and/or *Babiacetus*.

DISCUSSION

MUSM 3580 is the most complete skeleton of a quadrupedal (non-pelagicete) cetacean outside Indo-Pakistan. It constitutes one of the oldest, if not the oldest, quadrupedal cetacean from the New World (see [4]) and the first indisputable record for the whole Pacific Ocean and Southern Hemisphere. The new taxon shares similarities with several early protocetids from Indo-Pakistan (e.g., *Maiacetus* and *Rodhocetus*) at the level of the postcranial skeleton, including relative size and proportions of fore- and hind limbs, as well as several other plesiomorphic features (at least two fused sacrals, large articulation surface for sacral S1 on the innominate, relatively large ischiatic table, distinct fovea capita femoris, and retention of small hooves on both manus and pes). All these shared features suggest similar

terrestrial locomotion abilities for this younger protocetid from the Pacific Ocean, with the hind limbs capable of bearing the weight of the body on land [1] (Figures 2 and S4). In addition, the presence of large pes with elongated fingers and the dorso-plantar flattening of the phalanges with conspicuous lateral flanges indicating webbed pes (also observed on manus) suggest that hind limbs were actively used for swimming. Propulsive movements were either alternate or simultaneous hind-limb paddling or body and tail undulations, as observed in modern river and sea otters, alternating between lift-based propulsion via pelvic undulations, including tail and hind limbs, and drag-based propulsion via independent strokes of the hind limbs [26, 27] (Figures 2 and S4). The anatomy of the caudal vertebrae with expanded and bifurcated transverse processes is comparable to that of several semi-aquatic mammals, suggesting that the powerful tail was significantly involved during swimming, more so than in the geologically older *Maiacetus*, and illustrating thus a more derived stage in the gradual shift from drag-based to lift-based propulsion in early cetaceans [28]. In the beaver, this distinct morphology of the caudal vertebrae is restricted to the “scaly tail,” where firm collagenous tissue and numerous tendons produce a flattened, paddle-like distal tail. Pending the discovery of a more complete specimen, including posterior caudal vertebrae, it is not possible to determine whether *Peregocetus* possessed a well-developed tail fluke. In more derived protocetids, the innominate lost its articulation with the sacrum [11], before the strong reduction of the hind limb observed among basilosaurids [e.g., 29]. The moderately elongated snout (ratio between height of mandible posterior to p3 and total length estimated to 0.10) bearing robust anterior teeth with markedly ornamented enamel and shearing molars suggests that this large-size protocetid was capable of preying upon relatively large prey, for example large bony fish (Figure S4), an interpretation further supported by the incipient apical dental wear.

Several hypotheses have been proposed for the dispersal of protocetids to the New World: across the North Atlantic, along the coasts of Europe and the southern coast of Greenland, or via the west African coastline southward and then across South Atlantic [5–7] (Figure 4). Together with recent additions of fragmentary protocetid records from West Africa [7, 24, 25], the present report of a Lutetian South American protocetid, occupying a basal position in the protocetid phylogenetic tree and sharing features

with *Pappocetus* from the Bartonian of Morocco and Nigeria (step-like ventral margin of mandible and fovea capitis femoris; [14, 24]) further supports the hypothesis of an initial migration pathway across the South Atlantic [7] (Figure 4), before a northward dispersal to North America. Such a South Atlantic dispersal was made easier by the distance between Africa and South America being much shorter (more than two times) during the middle Eocene than today and the presence of a westward surface paleo-current from Africa to South America [30], both physical features having most likely also played a role in the westward dispersal of terrestrial mammals, for example primates and rodents [31, 32]. Although an eastward migration directly from the Asian center of origin of cetaceans to the southeastern Pacific cannot be completely ruled out, based on our current knowledge, this scenario appears much less likely, taking account of (1) the much longer distance either across the Pacific Ocean or along its coasts, (2) the absence of any protocetid record along the northern and southwestern coasts of the Pacific, and (3) the stronger morphological similarities between *Peregocetus* and fragmentarily known protocetid taxa from northwestern Africa, as noted above.

Protocetids are thus the first cetaceans to disperse as far as the Pacific Ocean, colonizing most epicontinental seas at low latitudes, nearly reaching a circum-tropical distribution while retaining functional, weight-bearing hind limbs, and only crossing the Tropic of Cancer along the eastern coast of the United States. Protocetids' descendants, basilosaurids and the modern lineages Mysticeti (baleen whales and relatives) and Odontoceti (echolocating toothed whales), then gradually migrated farther north and south, to finally reach a truly global distribution. Better preserved protocetid material from the Lutetian of Western Africa and North America will be needed to further investigate the different dispersal phases of these early quadrupedal whales to the Americas.

STAR★METHODS

Detailed methods are provided in the online version of this paper and include the following:

- KEY RESOURCES TABLE
- CONTACT FOR REAGENT AND RESOURCE SHARING
- EXPERIMENTAL MODEL AND SUBJECT DETAILS
- METHOD DETAILS
 - Geological Context
 - Calcareous Nannofossil Biostratigraphy and Geochronological Implications
 - Phylogenetic Analysis
 - Institutional Abbreviations
- DATA AND SOFTWARE AVAILABILITY

SUPPLEMENTAL INFORMATION

Supplemental Information can be found online at <https://doi.org/10.1016/j.cub.2019.02.050>.

A video abstract is available at <https://doi.org/10.1016/j.cub.2019.02.050#mmc5>.

ACKNOWLEDGMENTS

We thank W. Aguirre, A. Altamirano-Sierra, E. Díaz, K. Post, N. Valencia, and R. Varas-Malca for their help during fieldwork in November 2011; W. Aguirre

for the careful preparation of MUSM 3580; R. Varas-Malca for giving access to the MUSM collection; A. Gennari for preparing the life reconstructions of *Peregocetus pacificus*; J.H. Geisler for providing the nexus version of his recently updated morphological character-taxon matrix; M.D. Uhen for preliminary discussions on protocetid anatomy, for encouraging the study of this specimen, and for his contribution to the Paleobiology Database; and four anonymous reviewers for their constructive comments. Field expedition during which the skeleton MUSM 3580 has been collected was funded by the Muséum National d'Histoire Naturelle, Paris (Action Transversale "Biodiversité Actuelle et Fossile" 2011). Geological and stratigraphical field investigations were supported by a grant of the Italian Ministero dell'Istruzione dell'Università e della Ricerca (PRIN Project 2012YSBMK).

AUTHOR CONTRIBUTIONS

M.U. discovered the specimen MUSM 3580; C.d.M., G.B., M.U., O.L., and R.S.-G. took part to the excavation of the skeleton; C.D.C. analyzed the geological context and elaborated the stratigraphical section; E.S. undertook the biostratigraphical analyses; O.L. performed the phylogenetic analysis with input from C.d.M. and G.B.; C.D.C. and O.L. prepared the figures with input from C.d.M., E.S., G.B., and R.S.-G.; and O.L. wrote the manuscript with input from all authors.

DECLARATION OF INTERESTS

The authors declare no competing interests.

Received: January 21, 2019

Revised: February 20, 2019

Accepted: February 21, 2019

Published: April 4, 2019

REFERENCES

1. Gingerich, P.D., Haq Mu, Zalmout, I.S., Khan, I.H., and Malkani, M.S. (2001). Origin of whales from early artiodactyls: hands and feet of Eocene Protocetidae from Pakistan. *Science* 293, 2239–2242.
2. Thewissen, J.G.M., Williams, E.M., Roe, L.J., and Hussain, S.T. (2001). Skeletons of terrestrial cetaceans and the relationship of whales to artiodactyls. *Nature* 413, 277–281.
3. Thewissen, J.G.M., Cooper, L.N., Clementz, M.T., Bajpai, S., and Tiwari, B.N. (2007). Whales originated from aquatic artiodactyls in the Eocene epoch of India. *Nature* 450, 1190–1194.
4. Uhen, M.D. (2014). New specimens of Protocetidae (Mammalia, Cetacea) from New Jersey and South Carolina. *J. Vertebr. Paleontol.* 34, 211–219.
5. Uhen, M.D. (1999). New species of protocetid archaeocete whale, *Ecocetus wardii* (Mammalia: Cetacea) from the middle Eocene of North Carolina. *J. Paleontol.* 73, 512–528.
6. Geisler, J.H., Sanders, A.E., and Luo, Z.-X. (2005). A new protocetid whale (Cetacea: Archaeoceti) from the late middle Eocene of South Carolina. *Am. Mus. Novit.* 3480, 1–65.
7. Mourlam, M.J., and Orliac, M.J. (2018). Protocetid (Cetacea, Artiodactyla) bullae and petrosals from the Middle Eocene locality of Kpogamé, Togo: new insights into the early history of cetacean hearing. *J. Syst. Palaeontology* 16, 621–644.
8. Gingerich, P.D., Ul-Haq, M., von Koenigswald, W., Sanders, W.J., Smith, B.H., and Zalmout, I.S. (2009). New protocetid whale from the middle eocene of pakistan: birth on land, precocial development, and sexual dimorphism. *PLoS ONE* 4, e4366.
9. Lambert, O., Martínez-Cáceres, M., Bianucci, G., Di Celma, C., Salas-Gismondi, R., Steurbaut, E., Urbina, M., and de Muizon, C. (2017). Earliest mysticete from the Late Eocene of Peru sheds new light on the origin of baleen whales. *Curr. Biol.* 27, 1535–1541.e2.
10. Agnini, C., Fornaciari, E., Raffi, I., Catanzariti, R., Pálke, H., Backman, J., and Rio, D. (2014). Biozonation and biochronology of Paleogene

- calcareous nannofossils from low and middle latitudes. *Newsl. Stratigr.* 47, 131–181.
11. Hulbert, R.C., Jr., Petkewich, R.M., Bishop, G.A., Bukry, D., and Aleshire, D.P. (1998). A new middle Eocene protocetid whale (Mammalia: Cetacea: Archaeoceti) and associated biota from Georgia. *J. Paleontol.* 72, 907–927.
 12. McLeod, S.A., and Barnes, L.G. (2008). A new genus and species of Eocene protocetid archaeocete whale (Mammalia, Cetacea) from the Atlantic Coastal Plain. *Nat. Hist. Mus. of LA County Contrib. Sci.* 41, 73–98.
 13. Uhen, M.D. (2014). New material of *Natchitochia jonesi* and a comparison of the innominate and locomotor capabilities of Protocetidae. *Mar. Mamm. Sci.* 30, 1029–1066.
 14. Andrews, C. (1919). A description of new species of zeuglodont and of leathery turtle from the Eocene of southern Nigeria. *J. Zool.* 89, 309–319.
 15. Bianucci, G., and Gingerich, P.D. (2011). *Aegyptocetus tarfa*, n. gen. et sp. (Mammalia, Cetacea), from the middle Eocene of Egypt: clinorhynch, olfaction, and hearing in a protocetid whale. *J. Vertebr. Paleontol.* 31, 1173–1188.
 16. Uhen, M.D., Pyenson, N.D., DeVries, T.J., Urbina, M., and Renne, P.R. (2011). New middle Eocene whales from the Pisco Basin of Peru. *J. Paleontol.* 85, 955–969.
 17. Bebej, R.M., Zalmout, I.S., Abed El-Aziz, A.A., Antar, M.S.M., and Gingerich, P.D. (2016). First remingtonocetid archaeocete (Mammalia, Cetacea) from the middle Eocene of Egypt with implications for biogeography and locomotion in early cetacean evolution. *J. Paleontol.* 89, 882–893.
 18. Carlson, M., and Welker, W.I. (1976). Some morphological, physiological and behavioral specializations in North American beavers (*Castor canadensis*). *Brain Behav. Evol.* 13, 302–326.
 19. Amson, E., Argot, C., McDonald, H.G., and de Muizon, C. (2015). Osteology and functional morphology of the axial postcranium of the marine sloth *Thalassocnus* (Mammalia, Tardigrada) with paleobiological implications. *J. Mamm. Evol.* 22, 473–518.
 20. Hulbert, R.C., Jr. (1998). Postcranial osteology of the North American middle Eocene protocetid *Georgiacetus*. In *The Emergence of Whales*, J.G.M. Thewissen, ed. (New York: Plenum Press), pp. 235–267.
 21. Uhen, M.D. (2010). The origin(s) of whales. *Annu. Rev. Earth Planet. Sci.* 38, 189–219.
 22. de Muizon, C., and McDonald, H.G. (1995). An aquatic sloth from the Pliocene of Peru. *Nature* 375, 224–227.
 23. Ji, Q., Luo, Z.-X., Yuan, C.-X., and Tabrum, A.R. (2006). A swimming mammaliaform from the Middle Jurassic and ecomorphological diversification of early mammals. *Science* 311, 1123–1127.
 24. Gingerich, P.D., and Zouhri, S. (2015). New fauna of archaeocete whales (Mammalia, Cetacea) from the Bartonian middle Eocene of southern Morocco. *J. Afr. Earth Sci.* 111, 273–286.
 25. Gingerich, P.D., and Cappetta, H. (2014). A new archaeocete and other marine mammals (Cetacea and Sirenia) from lower middle Eocene phosphate deposits of Togo. *J. Paleontol.* 88, 109–129.
 26. Williams, T.M. (1989). Swimming by sea otters: adaptations for low energetic cost locomotion. *J. Comp. Physiol. A Neuroethol. Sens. Neural Behav. Physiol.* 164, 815–824.
 27. Fish, F.E. (1994). Association of propulsive swimming mode with behavior in river otters (*Lutra canadensis*). *J. Mammal.* 75, 989–997.
 28. Fish, F.E. (1996). Transitions from drag-based to lift-based propulsion in mammalian swimming. *Am. Zool.* 36, 628–641.
 29. Gingerich, P.D., Smith, B.H., and Simons, E.L. (1990). Hind limbs of eocene *basilosaurus*: evidence of feet in whales. *Science* 249, 154–157.
 30. Berggren, W.A., and Hollister, C.D. (1974). Paleogeography, paleobiogeography and the history of circulation in the Atlantic Ocean. In *Studies in Palaeo-Oceanography*, vol. 20, W.H. Hay, ed. (SEPM Society for Sedimentary Geology), pp. 126–186.
 31. de Oliveira, F.B., Molina, E.C., and Marroig, G. (2009). Paleogeography of the South Atlantic: a route for primates and rodents into the New World? In *South American primates: comparative perspectives in the study of behavior, ecology, and conservation*, P.A. Garber, A. Estrada, J.C.B. Bicca-Marques, E.W. Heymann, and K.B. Strier, eds. (Springer), pp. 55–68.
 32. Antoine, P.-O., Marivaux, L., Croft, D.A., Billet, G., Ganerød, M., Jaramillo, C., Martin, T., Orliac, M.J., Tejada, J., Altamirano, A.J., et al. (2012). Middle Eocene rodents from Peruvian Amazonia reveal the pattern and timing of caviomorph origins and biogeography. *Proc. Biol. Sci.* 279, 1319–1326.
 33. Gibson, M.L., Mnieckowski, J., and Geisler, J.H. (2019). *Tupelocetus palmeri*, a new species of protocetid whale (Mammalia, Cetacea) from the Middle Eocene of South Carolina. *J. Vertebr. Paleontol.* Published online March 19, 2019. <https://doi.org/10.1080/02724634.2018.1555165>.
 34. Swofford, D.L. (2001). *Phylogenetic analysis using parsimony (and other methods)*. Version 4b10 (Sunderland: Sinauer Associates).
 35. Maddison, W.P., and Maddison, D.R. (2018). *Mesquite: a modular system for evolutionary analysis*. Version 3.51. <http://www.mesquiteproject.org>.
 36. Thornburg, T.M., and Kulm, L.D. (1981). Sedimentary basins of the Peru continental margin: structure, stratigraphy, and Cenozoic tectonics from 6°S to 16°S latitude. In *Nazca Plate: Crustal Formation and Andean Convergence*, vol. 154, L.D. Kulm, J. Dymond, E.J. Dasch, and D.M. Hussong, eds. (Geological Society of America), pp. 393–422.
 37. Dunbar, R.B., Marty, R.C., and Baker, P.A. (1990). Cenozoic marine sedimentation in the Sechura and Pisco basins, Peru. *Palaeogeogr. Palaeoclimatol. Palaeoecol.* 77, 235–261.
 38. Mukasa, S.B., and Henry, D.J. (1990). The San Nicolás Batholith: early Palaeozoic continental arc or continental rift magmatism? *J. Geol. Soc. London* 147, 27–39.
 39. DeVries, T.J. (1998). Oligocene deposition and Cenozoic sequence boundaries in the Pisco Basin (Peru). *J. S. Am. Earth Sci.* 11, 217–231.
 40. DeVries, T.J. (2017). Eocene stratigraphy and depositional history near Puerto Caballas (East Pisco Basin, Peru). *Bol. Soc. Geol. Peru* 112, 39–52.
 41. DeVries, T.J., Urbina, M., and Jud, N.A. (2017). The Eocene-Oligocene Otuma depositional sequence (East Pisco Basin, Peru): paleogeographic and paleoceanographic implications of new data. *Bol. Soc. Geol. Peru* 112, 14–38.
 42. DeVries, T.J., and Jud, N.A. (2018). Lithofacies patterns and paleogeography of the Miocene Chilcatay and lower Pisco depositional sequences (East Pisco Basin, Peru). *Bol. Soc. Geol. Peru* 8, 124–167.
 43. Di Celma, C., Malinverno, E., Bosio, G., Collareta, A., Gariboldi, K., Gioncada, A., Molli, G., Basso, D., Varas-malca, R.M., Pierantoni, P.P., et al. (2017). Sequence stratigraphy and paleontology of the Upper Miocene Pisco Formation along the western side of the lower Ica Valley (Ica Desert, Peru). *Riv. Ital. Paleontol. Stratigr.* 123, 255–273.
 44. Gariboldi, K., Bosio, G., Malinverno, E., Gioncada, A., Di Celma, C., Villa, I.M., Urbina, M., and Bianucci, G. (2017). Biostratigraphy, geochronology and sedimentation rates of the upper Miocene Pisco Formation at two important marine vertebrate fossil-bearing sites of southern Peru. *Newsl. Stratigr.* 50, 417–444.
 45. Azalgará, C. (1994). Structural evolution of the offshore forearc basins of Peru, including the Salaverry, Trujillo, Lima, West Pisco and East Pisco Basins. Master thesis (Rice University).
 46. Steurbaut, E., and King, C. (1994). Integrated stratigraphy of the Mont-Panisel borehole section (151E340), Ypresian (Early Eocene) of the Mons Basin, SW Belgium. *Bull. - Soc. Belge Géol.* 102, 175–202.
 47. Steurbaut, E., and Sztrákos, K. (2008). Danian/Selandian boundary criteria and North Sea Basin-Tethys correlations based on calcareous nannofossil and foraminiferal trends in SW France. *Mar. Micropaleontol.* 67, 1–29.

48. Bown, P.R., and Dunkley Jones, T. (2006). New Palaeogene calcareous nanofossil taxa from coastal Tanzania: Tanzania Drilling Project Sites 11 to 14. *J. Nanoplankton Res.* 28, 17–34.
49. Martini, E. (1971). Standard Tertiary and Quaternary calcareous nanoplankton zonation. In *Proceedings of the Second Planktonic Conference*, 2, pp. 739–785.
50. Perch-Nielsen, K. (1985). Cenozoic calcareous nanofossils. In *Plankton Stratigraphy*, H.M. Bolli, J.B. Saunders, and K. Perch-Nielsen, eds. (Cambridge University Press), pp. 427–554.
51. Bown, P.R. (2005). Palaeogene calcareous nanofossils from the Kilwa and Lindi areas of coastal Tanzania (Tanzania Drilling Project 2003-4). *J. Nanoplankton Res.* 27, 21–95.

STAR★METHODS

KEY RESOURCES TABLE

REAGENT or RESOURCE	SOURCE	IDENTIFIER
Deposited Data		
Character-taxon matrix	This paper; [33]	https://morphobank.org/permalink/?P3380
Software and Algorithms		
PAUP 4.0a150	[34]	http://phylosolutions.com/paup-test/
Mesquite 3.51	[35]	http://www.mesquiteproject.org

CONTACT FOR REAGENT AND RESOURCE SHARING

Further information and requests for resources and reagents should be directed to and will be fulfilled by the Lead Contact, Olivier Lambert (olivier.lambert@naturalsciences.be).

EXPERIMENTAL MODEL AND SUBJECT DETAILS

The fossil specimen analyzed in this work (MUSM 3580) was discovered and excavated during a fieldwork campaign in the Pisco Basin (locality Playa Media Luna) in November 2011. The collected bones were brought to the Museo de Historia Natural, Universidad Nacional Mayor de San Marcos (Lima, Peru) for mechanical preparation and curation.

METHOD DETAILS

Geological Context

According to [36], two structurally-controlled, trench-parallel basement highs were formed on the continental shelf and upper slope of the Peruvian margin during late Cretaceous-early Paleogene time, namely the Outer Shelf High (OSH) and the Upper Slope Ridge (USR). These two highs dissected the Peruvian offshore resulting into a series of paired shelf and upper slope forearc basins.

In southern Peru, the present-day onshore portion of the East Pisco Basin is separated from the adjacent offshore West Pisco Basin by the Coastal Cordillera, the onshore extension of the submerged OSH. The two basins experienced a similar tectonostratigraphic evolution through middle Eocene-Pliocene times and are inferred to share many similarities. The Cenozoic succession exposed in the East Pisco Basin [37] is underlain by Mesozoic and older crystalline and metasedimentary basement rocks [36, 38] and is punctuated by several stratigraphic breaks of various magnitudes. Its stratigraphic framework was first established by DeVries [39], who subdivided the basin fill into five formations separated by basin-wide unconformities: 1) the Eocene Caballas and Paracas formations, the latter including the Los Choros and Yumaque members (see [40] for an explanation about the decision to downgrade the Los Choros and Yumaque formations of previous authors to members of the Paracas Formation); 2) the uppermost Eocene to lower Oligocene Otuma Formation [41]; 3) the upper Oligocene to lower Miocene Chilcatay Formation [42]; and 4) the (?) middle Miocene to lower Pliocene Pisco Formation [43, 44].

Most of the West Pisco Basin lies offshore, with a small portion of its eastern margin exposed onshore along the seaward side of the Coastal Cordillera/OSH. Notwithstanding its Cenozoic sedimentary record is little explored, the “E3” and “E-O” seismic sequences documented by [45] in the West Pisco Basin are thought to be correlative with the Los Choros and Yumaque members of the Paracas Formation, respectively [40].

In September 2015, a 150 m-thick lithological section of Eocene strata of the West Pisco succession was measured in a coastal outcrop adjacent to Media Luna Bay, on the seaward side of the Coastal Cordillera/OSH. The measured succession comprises shallow-water, medium- to coarse-grained, massive and cross-laminated bioclastic sandstones, assigned to the upper part of the Los Choros Member, gradually overlain by offshore, finely laminated or massive, green-gray diatomaceous siltstones rich in fish scales, assigned to the Yumaque Member. Thirty-four samples for micropaleontological analyses were collected from this outcrop section during the 2015 fieldwork campaign and their stratigraphic position with respect to that of the protocetid specimen described in this study is shown in Figure S1.

Calcareous Nannofossil Biostratigraphy and Geochronological Implications

Material and methods

The stratigraphic investigation of the *Peregoctes pacificus* discovery in the Media Luna area of SW Peru is part of an overall study of marine mammal evolution in the eastern Pacific Ocean during middle and late Eocene times [9]. It is based on a high-resolution

calcareous nannofossil analysis of 40 samples, 38 of which are almost evenly spaced over the about 128 m thick Yumaque Member and the lower 16 m of the overlying Otuma Formation. The lowermost two were taken at the top of the Los Choros Member. Samples (ML13-0a to ML13-4 and ML1 to ML34, collected in 2013 and 2015 respectively, [Table S1](#)) were processed following the preparation and investigation procedures explained by Steurbaut and King [46] and Steurbaut and Sztrákos [47]. The CNE (Calcareous Nannofossil Eocene) biozonation of Agnini et al. [10], the upper part of which (CNE10 to CNE21) is defined in the central western Atlantic ODP Sites 1051 and 1052 and the southeastern Atlantic DSDP Site 522, is applied herein. Additional biohorizons used to specify or subdivide the middle Eocene interval in these Atlantic borehole sections [10] and in other low latitude borehole sections (e.g., onshore Tanzania [48]) have also been recorded, allowing a high-resolution dating. Among these, are the HO of *Discoaster bifax*, falling within CNE12 (although note that the information on p. 159 of Agnini et al. [10] is not in line with that on Figure 13) and the presence of *Sphenolithus strigosus*, which according to Bown and Dunkley Jones [48] is restricted to standard nannofossil zone NP16 of Martini [49]. The age estimates of the biohorizons are taken from [10]. The taxonomy is essentially from [50], taking into account the subsequent additions by [51] and [48]. Rock samples and microscopic slides are stored at the Royal Belgian Institute of Natural Sciences (RBINS), Brussels, Belgium. The following abbreviations are used in text and table: LO = lowest occurrence, HO = highest occurrence, mod. = moderately, pres. = preserved or preservation, r. = rather, Fm = Formation, Ma = million years ago, Mb = Member.

Biozonation, dating and sedimentation rates in the Yumaque Member

As already discussed in [9], the Yumaque Mb is bracketed between the LO of *Criboecentrum reticulatum* below (1 specimen recorded at 2 m above its base; lower 2 m with badly preserved nannofossil assemblages) and the HO of *Discoaster saipanensis* above (present at 6 m below its top, but absent at 5 m above its top, and no nannofossil records in between). Accordingly, it would range from the upper part of zone CNE13 to the lower part of zone CNE21 of Agnini et al. [10], or equally possibly, terminating in the underlying zone CNE20. Hence, the lower boundary of the Yumaque Mb should lie at approximately 42.8 Ma (based on the calculated accumulation rates, see below) and its upper boundary at 34.4 Ma. Apparently, it took about 8.4 myr to deposit this ca 127.65 m thick unit, which implies a mean sedimentation rate of 1.5 cm/kyr. Sedimentation rates are not constant throughout the Yumaque Mb, as shown by the estimated nannofossil-based ages recorded within the unit. An about 24 m thick succession (from 4 m to 28 m above base Yumaque Mb, see [Table S1](#)) was laid down during the about 2 million-year-long Biochron CNE14 [10], indicating a sedimentation rate of 1.2 cm/kyr in the lowermost 28 m. Rates seem to be progressively increasing during deposition of the member from 1.2 cm/kyr in the lowermost 28 m, through 2.0 cm/kyr in the interval from 40 m to 62.5 m, to 2.5 cm/kyr in the uppermost 65 m of the Yumaque Mb, except for a substantial decrease to 0.6 cm/kyr in the interval from 28.85 m to 40 m.

Age of the MUSM 3580-bearing bed.

The skeletal remains of *Peregocetus pacificus* MUSM 3580 were unearthed at 1.95 m above the base of the Yumaque Mb ([Figure S1](#), [Table S1](#)), within an interval with moderately to rather well-preserved calcareous nannofossil assemblages. The highest diversity has been encountered at 0.5 m above MUSM 3580, in an assemblage dominated by small Noelarhabdaceae and by rather large Coccolithaceae. Large-sized *Reticulofenestra umbilica* (several with a diameter larger than 16 μm , even up to 20 μm) and large-sized *Coccolithus pelagicus* (several with $D > 20 \mu\text{m}$) are quite common, as well as *Coccolithus formosus*, and to a lesser degree, *Pontosphaera* spp. and *Helicosphaera* spp. *Sphenolithus* taxa are consistently present, although in low numbers, including *S. furcatolithoides* forma B (known to occur from CNE12 to CNE14), *S. strigosus* (restricted to Martini's Zone NP16 [48]) and a new species of *Sphenolithus* (informally named *S. sagittatus*). An almost identical, but much more impoverished assemblage is recorded just below MUSM 3580. The common presence of large-sized *R. umbilica*, associated with the rare occurrence of *Criboecentrum reticulatum* (only 1 specimen encountered in the interval immediately below and above MUSM 3580) and the absence of the *Nannotetrina alata* group, *Helicosphaera compacta* and *Dictyococcites bisectus*, indicates the upper part of Zone CNE13 of Agnini et al. [10]. This would mean that *P. pacificus* MUSM 3580 fossilized during the early late Lutetian, at the end of Chron C20n, approximately 42.6 Ma ago.

Phylogenetic Analysis

To investigate the phylogenetic relationships of *Peregocetus* with other early cetaceans, MUSM 3850 was coded in the morphological matrix of Gibson et al. [33], modified from [6] and [13] (see [Data S1](#)). The cladistic analyses were undertaken with Paup 4.0 [34]. Because first tests with the complete list of taxa yielded poorly resolved relationships in some parts of the tree, we removed five more fragmentarily known taxa from the analysis. Heuristic searches were performed with and without downweighting of homoplastic characters (DHC, with $K = 3$), before strict consensus trees were calculated ([Figures 3 and S3](#)). Bootstrap support values were calculated with Paup 4.0 (500 replicates).

To identify the main dispersal events during early cetacean paleobiogeographic history, we mapped locality data for all the taxa on the consensus tree of the analysis with DHC, optimizing this biogeographic character using the software Mesquite 3.51 [35]. Five main geographic areas were considered: India + Pakistan, North Africa, South America, east coast USA, and northern Europe ([Figure 4](#)), and the character was treated as unordered.

Institutional Abbreviations

MUSM, Museo de Historia Natural, Universidad Nacional Mayor de San Marcos, Lima, Peru

DATA AND SOFTWARE AVAILABILITY

Our character-taxon matrix is deposited on the MorphoBank website, under the project number 3380, at the following address:
<https://morphobank.org/permalink/?P3380>